Pyxis®: Enhanced Thermal Imaging with a Division of Focal Plane Polarimeter

15 September 2015

David Chenault, Larry Pezzaniti, Justin Vaden, Michael Roche
Polaris Sensor Technologies, Inc.
200 Westside Square, Suite 320
Huntsville, AL 35801

Jacob Michalson,
Armaments Research, Development and Engineering Center,
Building 44
Picatinny Arsenal, NJ 07806-5000

Kristan Gurton
U.S. Army Research Laboratory, RDRL-CIE-S
2800 Powder Mill Road
Adelphi, MD 20783

Abstract

Polarization has long held the promise for adding detection and discrimination capability to conventional infrared (IR) systems and its use has been pursued for decades. Previous data collection efforts have shown significantly improved contrast of polarimetric signatures over that of infrared images of the same scene. The combination of polarization and infrared imagery offers still better contrast improvement for both algorithms and intuitive understanding of the scene by an operator. Application of polarimetric imagers has in the past been limited to less demanding data collection activities to accommodate the size and complexity of the sensors and data acquisition systems, and frequently due to the need to make sequential measurements leading to artifacts caused by image mis-registration. In this paper we report on the development of Pyxis®, a division of focal plane imaging polarimeter in which a polarizing filter operates in conjunction with a microbolometer focal plane array. The result is a snapshot imaging polarimeter in a compact, low power package that outputs realtime data in both analog and digital formats. Pyxis® is the same size and uses many of the same lenses as off-the-shelf microbolometers. Both IR performance (NEDT) and

polarization response (noise equivalent degree of linear polarization or NEDOLP) are comparable to existing sensors. The analog output is selected by the user to be conventional IR radiometric image (S0 of the Stokes vector), S1 and S2 of the Stokes vector, the degree of linear polarization, or a colorized fused image combining contrast from polarimetric and IR images. The digital data can be recorded, manipulated, and displayed on a laptop in realtime with additional data products and analytical capabilities. The integration process for the pixelated filter is amenable to volume manufacturing and hence offers a sensor comparable to current uncooled microbolometers with the enhanced polarization capability making the technology suitable for widespread deployment. Pyxis® represents a leap-ahead capability for intelligence, target acquisition, and engagement applications for ground targeting systems, unmanned aerial platforms, and even missiles and smart weapons. In this paper, we will describe the sensor and its performance, and show polarimetric video of representative scenarios.

Key Words: Polarization, Degree of Linear Polarization, target detection, Infrared polarimetry, imaging polarimetry, Stokes polarimeter

1.0 Introduction

It has been well established in the literature that imaging LWIR polarimetry provides a robust method for recovering contrast in scenes with low thermal variation[1,2] as shown in Figures 1 and 2. Polarimetric signatures have been shown to be stable throughout the diurnal cycle including demonstrating particular utility during instances of thermal cross-over[3]. Because it is fundamentally a physics-based approach for recovering image contrast, imaging polarimetry is particularly adept at distinguishing between man-made and naturally-occurring objects[4,5,6,7].

1.1. Polarization Overview

Polarization results from the vector nature of light. As light propagates along a given vector, the electric field oscillates sinusoidally along an axis that is orthogonal to the propagation axis, as described by the wave equation[8]. This oscillation can be described using four parameters: 1) the amplitude of the oscillation (i.e. the intensity), 2) the spacing between the peaks of the oscillation (i.e. wavelength), 3) the coherence of the oscillation, and 4) the angle between the axis of oscillation and horizontal axis (i.e. the polarization

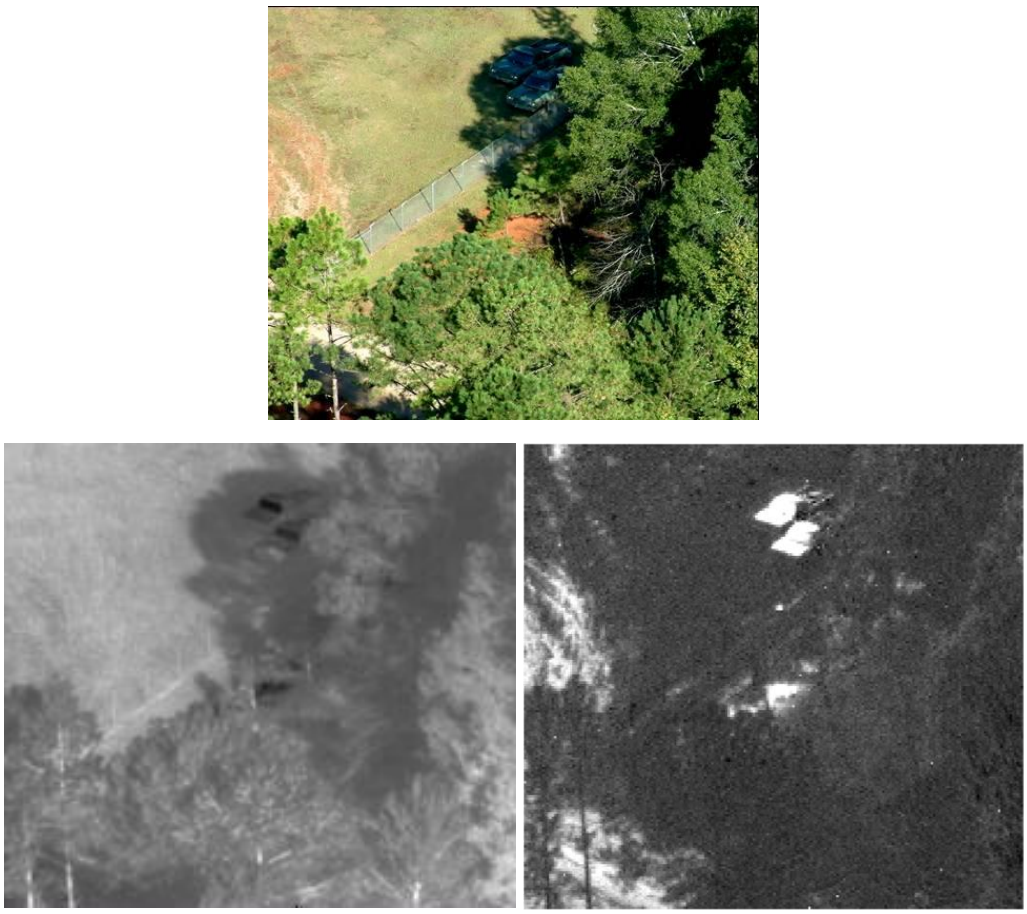

Figure 1. Visible picture of two pickup trucks in shade (top), long-wave IR intensity image (bottom left), and long-wave IR polarization image (bottom right). Strong contrast in the polarization image shows advantages for enhanced target detection using imaging polarimetry.

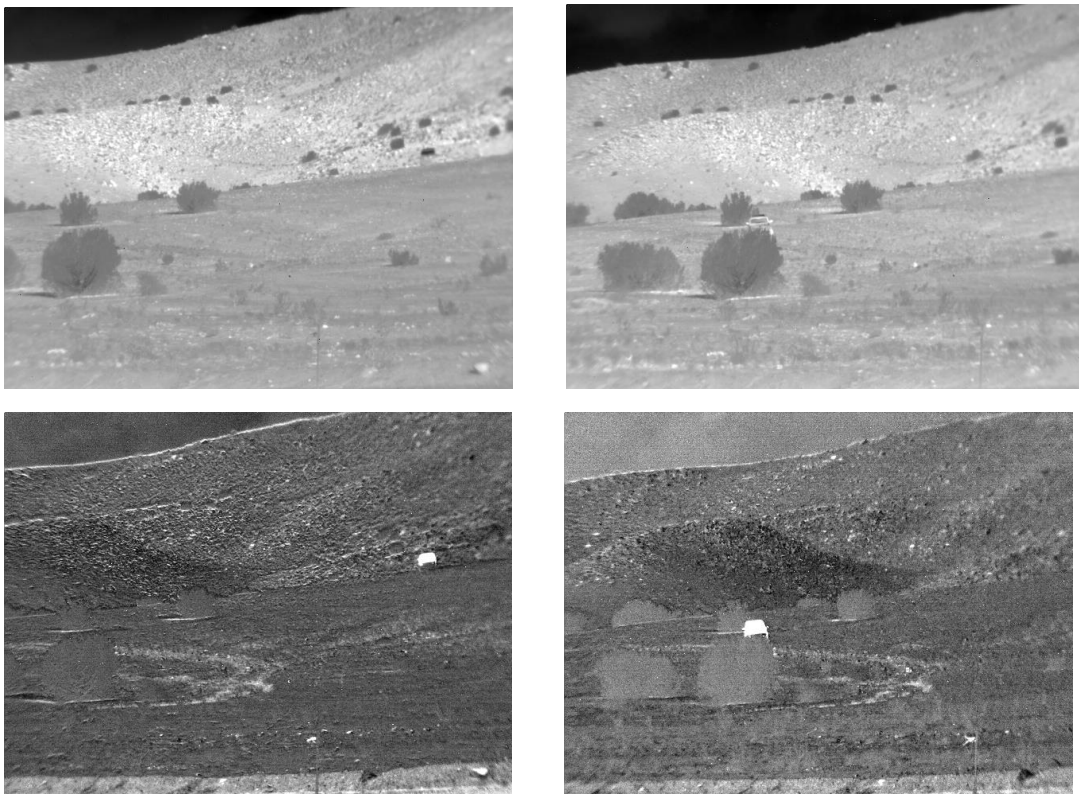

Figure 2. Conventional IR (top row) and polarimetric imager (bottom row) of the same scene. The polarimetric imagery clearly detects the vehicle and suppresses the background. In addition the polarization imagery brings out significant detail for the tracks and the berm in the foreground.

angle), as shown in **Error! Reference source not found.**3. Polarization is therefore a fundamental quantity of the propagating light wave just as intensity, wavelength, and coherence are also fundamental quantities.

As the wave interacts with a surface boundary (whether through reflection or emission), the surface preferentially passes one orientation of the e-field. Similarly the same surface will preferentially attenuate the orthogonal e-field orientation. The combination of these two actions produces polarized light. For emission, the surface preferentially emits an e-field that oscillates parallel to the surface normal (the opposite is true for reflection)[9]. The degree of preferential emission and preferential attenuation (i.e. the degree of polarization) is dependent on the smoothness of the surface and the angle of incidence (AOI) between the incident light and the surface[10]. Thus, for a polarimetric image, contrast between two surfaces occurs when there is a change in the surface roughness and/or AOI relative to the sensor.

As the oscillation of the e-field can be described using a vector, it is therefore possible to decompose that vector into its two orthogonal components. Typically, the orthogonal components used are the horizontal (parallel to the earth's surface) and vertical (perpendicular to the earth's surface). The comparison of horizontal and vertical is referred to as the S_1 parameter. Because S_1 is based on a comparison of horizontal and vertical, there are three special cases to consider: 1) all light is polarized at 45^o, 2) all light is polarized at 135^o, and 3) all light is equally distributed across all possible orientations (i.e. unpolarized light). Each of these three cases will produce an S_1 value of zero, even though the light is completely polarized in cases 1 and 2. To address this, a second standard parameter is used to compare 45^o and 135^o

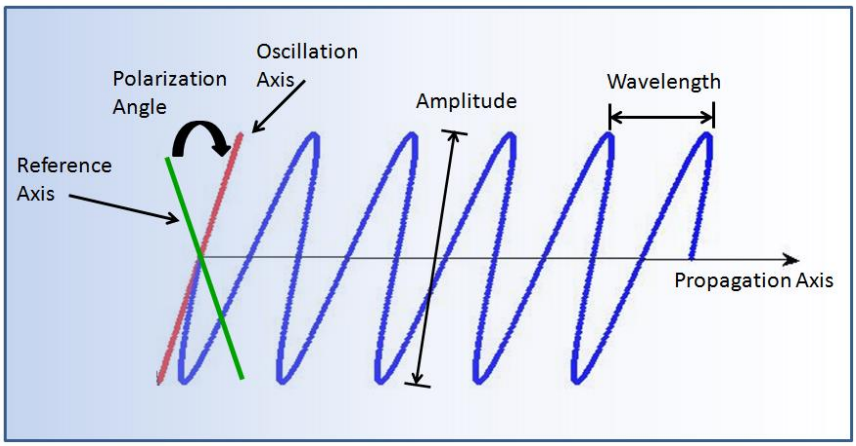

Figure 3. Polarization of propagating light wave

light, referred to as the S_2 parameter. Finally, the standard radiometric image is therefore simply the summation of orthogonal components from either S_1 or S_2.

Put together, the S_0, S_1, and S_2 parameters (collectively referred to as Stokes Parameters) provide a complete description of the orientation and amplitude of the incident thermal energy. One additional parameter, the Degree of Linear Polarization (DoLP), combines all the available polarimetric information into a single value. For the purposes of this paper, DoLP will serve as the polarimetric data product of interest for comparing polarimetry to the standard radiometric image. The functional form for these polarimetric data products can be found in Equations (1) through (4).

$$S_0 = H + V = 45 + 135 = .5 \cdot (H + 45 + V + 135) \quad \textbf{(1)}$$

$$S_1 = (H - V)/(H + V) = (H - V)/S_0 \quad \textbf{(2)}$$

$$S_2 = (45 - 135)/(45 + 135) = (45 - 135)/S_0 \quad \textbf{(3)}$$

$$DoLP = \sqrt{S_1^2 + S_2^2} \quad \textbf{(4)}$$

While S_0 is the standard thermal image and reports changes in intensity, the other three polarimetric data products can be regarded as a variation on Michelson's Contrast Formula and thus produce image contrast that is not dependent on intensity[11]. For this reason, the contrast obtained from S_1, S_2, and/or DoLP can be fused with the thermal image to create an Enhanced Thermal (eTherm) image that leverages all available information to generate a more-complete representation of the scene. Because S_0, S_1, S_2, and DoLP are all generated simultaneously for each output frame, the eTherm image is therefore simultaneously generated as well.

1.2. Polarimetric Imaging

There are a number of methods for acquiring polarimetric imagery[12]. Since polarimetric imaging is effectively adding an additional dimension to the acquired data, the real world dimensions have to be divided in some way to measure polarization. Thus the terminology of the four most common ways to

perform polarimetric imaging are termed division of time, division of amplitude, division of aperture, and division of focal plane.

A division of time polarimeter collects polarimetric information as a function of time typically by rotating a polarization filter (polarizer or retarder). This approach can also be done through polarimetric modulation such as with a liquid crystal retarder. The disadvantage of this approach is that both the scene and the sensor must remain stable over the course of the data collection, and if not, polarization artifacts are generated from any motion of the sensor or scene elements. This is not satisfactory for moving targets or when the sensor is on a moving platform.

A division of amplitude sensor splits the amplitude of the incoming light and directs the light on to separate focal planes. With a unique polarization filter in front of each focal plane, this allows for simultaneous capture at the full frame size of the focal planes, but is expensive (since it requires at least three focal plane arrays or FPAs) and is large and power hungry. Image registration must also be carefully done mechanically, in software, or both.

A division of aperture system uses a single FPA and divides up the light through a reimaging system to produce multiple copies of the input scene on the focal plane. Each of the copies is filtered with a unique polarization state to provide the polarimetric information. This allows for simultaneous capture of the polarimetric data, and only requires a single focal plane, but the resolution of the captured image is reduced by half in each dimension. Therefore the chief disadvantage of this approach is the loss of resolution.

Finally, the division of focal plane approach for polarimetric imaging addresses many of the shortcomings of the previous three approaches. In this approach, a polarizing filter (which can include relay optical lenses) is used in conjunction with the focal plane array as shown in Figure 4. The polarizing filter is pixelated, meaning that polarizer orientations are changed from one pixel to the next, much in the same way that the color filters are changed in a Bayer filter. There is a one to one correspondence between a polarizing filter of a particular orientation and pixels on the focal plane. Through this approach, simultaneous capture is possible, only a single focal plane is used, and there is (through judicious use of interpolation) no loss of resolution. The single biggest disadvantage is that there is misregistration from one instantaneous field of

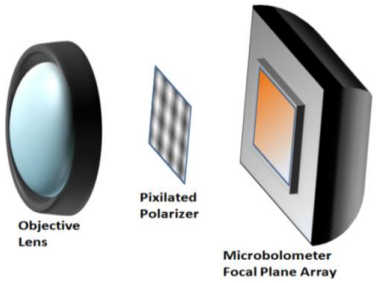

Figure 4. An infrared division of focal plane polarimeter employs a pixilated polarizer filter in conjunction with a microbolometer.

view (IFOV) to the next which limits the utility of this approach when looking at single pixel targets. However, the small sensor size and richer set of data products enabled by this architecture is significant for a large number of applications.

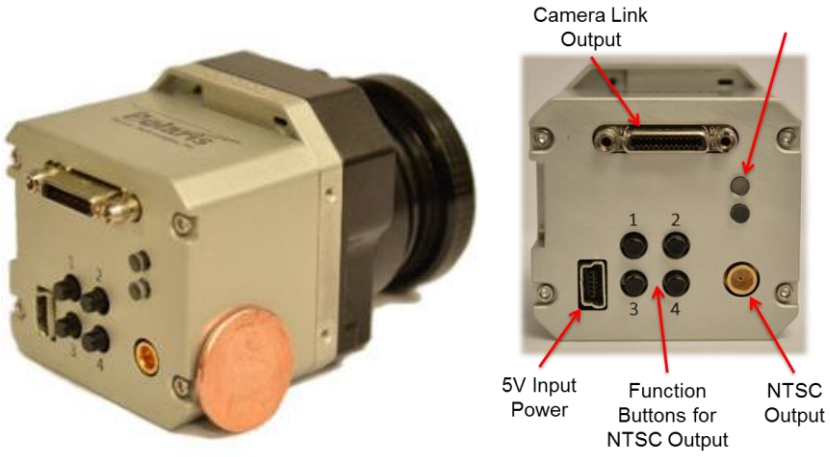

Figure 5. They Pyxis® LWIR 640 Imaging Polarimeter

2.0 Pyxis®

2.1. Sensor Description

Through SBIR Phase II Enhancement funding provided by the Army Research Laboratory and Picatinny Arsenal, we have developed Pyxis®, a division of focal plane polarimeter using a microbolometer as the underlying detector. Using the architecture shown in Figure 4, the integrated system is small, lightweight, and low power. The final integrated system is shown in Figure 5. The microbolometer has a 17 micron pixel pitch with 640 x 512 format. The pixelated filter array is the same format of the FPA and the full array is exploited. A proprietary interpolation scheme is used on the Stokes images (S_0, S_1, and S_2) so that the output polarization data product images are full format. The noise equivalent degree of polarization (NEDOLP) is less than 0.5% and is typically on the order of 0.2%. Some light is lost due to the polarization optics, but performance is equivalent to comparable microbolometers through the use of faster lenses. Other

Table 1: Pyxis® specifications

Detector	Uncooled VOx Microbolometer Array
Waveband	7.5 – 13 mm
Pixel Pitch	17 mm
Format	640 x 512 pixels
Frame Rate	30 Hz.
Full Frame Pixel Operability	> 99.9%
NEDT @ f/0.87	< 50 mK
NEDOLP	< 0.5%
Size (w/o lens)	1.79 x 1.75 x 1.79”
Weight w/o lens	83 grams
Input Voltage	5 V
Steady State Power @ 23°C	4 W
Peak Power @ 23°C	5.3
Data Interface	NTSC, 14-bit Camera Link, GigE

Table 2: Lenses currently available for Pyxis®

Focal Length	F/#	Field of View	Instantaneous FOV
20 mm	0.87	31° x 25°	0.85 mrad
25 mm	0.87	25° x 20°	0.68 mrad
50 mm	0.87	12.5° x 10°	0.34 mrad

specifications are shown in Table 1. Lens options available are shown in Table 2. Key parameters are the small size (1.79 x 1.75 x 1.79" or 5.6 cubic inches), low weight (83 grams without lens), and low power (4 watts). The small SWAP enables applications requiring helmet mounted sensors, integration into existing gimbals, or integration with small UAS.

On-board FPGA electronics provides real-time processed polarization products as well as standard thermal video. The Camera Link and analog outputs are shown in Figure 5, but gigabit Ethernet (GigE) is also an option. Both digital and analog output modes can be output at the same time, allowing for capture of the digital data for later manipulation while also providing analog output to a monitor. The four buttons are used to manipulate the analog output and provide five output data products (S_0, S_1, S_2, DoLP, and eTherm, described in greater detail below), provide one and two point non uniformity corrections (NUC), and adjust the dynamic range, or contrast, of the analog output.

In situations when the polarization signatures of targets are very strong but the rest of the scene is relatively unpolarized, the target polarimetric signatures can overwhelm the dynamic range of the image. An example showing this to some extent is given in Figure 1. In other instances, the S_0 image can frequently offer valuable target information. In either of these cases, it is less effective for human-in-the-loop understanding of the imagery to look at only one data product, and cumbersome to look at two images to capture all of the useful contrast. Since polarimetric data contains three potentially linear independent features (S_0, DoLP, and orientation for example), it is reasonable to fuse the data into a single image. Through the use of color, one can capture all independent aspects of the data in a single, colorized image[13] that enhances the conventional thermal image, hence the term eTherm. In this way, the intensity information in the thermal image is preserved, while the polarization-based coloring aids the operator in interpreting low-contrast scenes. One mapping for S_0, DoLP and orientation to the color parameters hue H, saturation S, and value V is given by[14]

$$H = \text{atan}(S2 / S1); \quad S = \text{DoLP}; \quad V = S_0, \qquad \textbf{(5)}$$

To see the efficacy of this fusing approach, the eTherm image is presented side-by-side with the standard thermal image in Figure 6. Note that only portions of the scene with a high degree of polarization are colorized whereas regions with low polarization automatically reduce to the same grayscale value present in the standard thermal image. Most importantly, as polarization is dependent on the physics of the scene, the color scheme is consistent from frame to frame.

For digital recording, Pyxis® Vision Science (PVS) software provides a flexible user interface to the operator. Using PVS as shown in Figure 7, polarimetric image data can be viewed live to allow the operator to set up a recording session. Live data continues to be displayed while recording is occurring at whatever the image data bandwidth allows to ensure no frames are missed in the recorder pipeline. Live data display can be set to either the raw camera data, or to a variety of processed data products using standard image

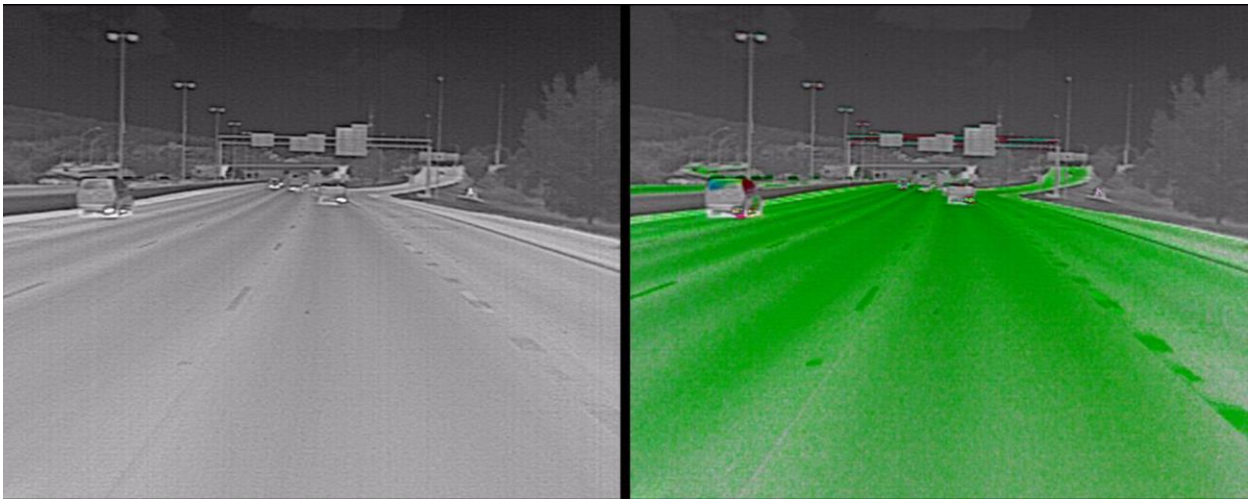

Figure 6. Thermal image (left) and eTherm image (right) from Pyxis®.

processing filters, or sensor specific data reduction algorithms. A variety of grayscale and false color mappings, including eTherm, are available to assist in interpreting the sensor data on the screen. Image statistics are available for the entire image, or for user defined Regions of Interest (ROI).

PVS allows the user to determine the method of data recording. Raw data may be streamed to the disk by the user manually using the graphical data recorder interface. The user may also choose to use the scripted Periodic & Event Recorder which allows for a great deal of flexibility in how data is recorded. Using the Periodic & Event Recorder the user defines a sequence of Record Windows. These Record Windows define the frame rate and number of frames to record. The Periodic & Event Recorder will execute these windows periodically or at user specified times. The Periodic & Event Recorder allows the user to collect only that data that is of critical importance without having to store terabytes of data or having to be present with the sensor to manually record the event.

2.2. Representative Data

Figures 8 and 9 show more representative data demonstrating the effectiveness of polarimetric imaging for target detection and clutter suppression. Figure 8 is a street scene with parked cars, sidewalks and driveways highlighted with their polarization signatures. Improved situational awareness and clutter rejection result from the colorized scene.

Figure 9 shows a parking lot scene in which several cars are not readily apparent from the thermal image. An alternate color scheme is used for the eTherm image on the right. In this image, two cars that are partially obscured by trees are easily detectable in the eTherm image and a third car that has limited thermal contrast is easily detectable as well.

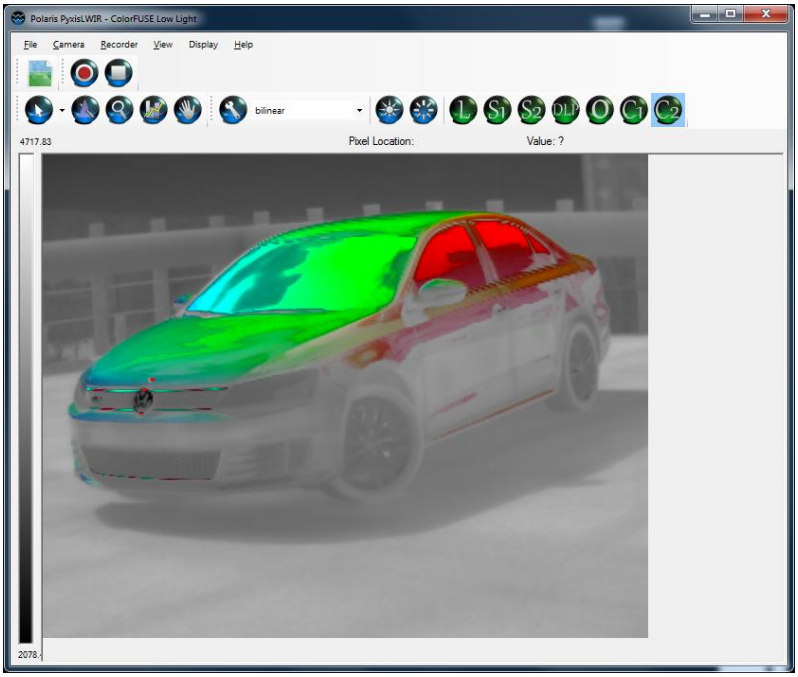

Figure 7. Pyxis® Vision Science interface for recording and analyzing polarimetric data from Pyxis®. The buttons across the top right provide quick access to polarimetric data products. C_1 and C_2 are two different color schemes for eTherm imagery.

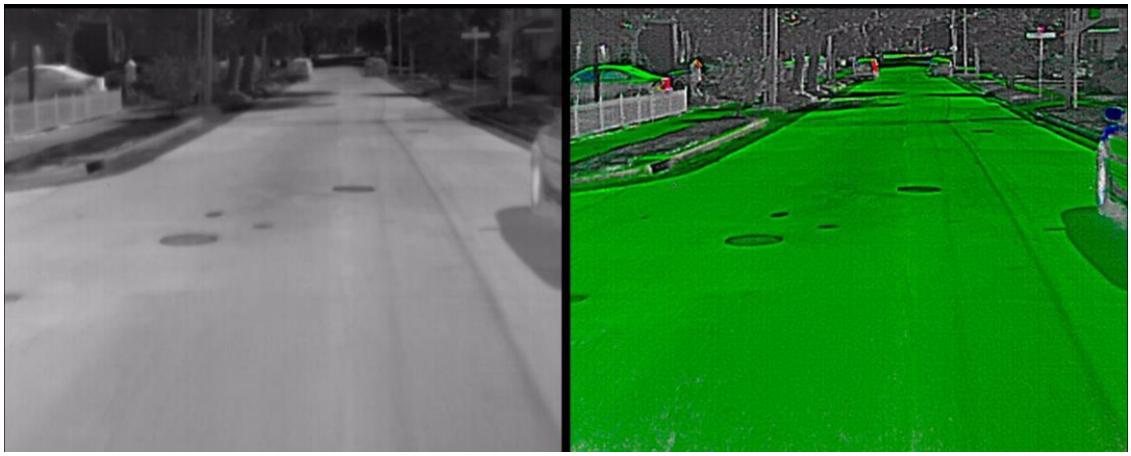

Figure 8. Thermal (left) and polarimetric eTherm (right) imagery. The eTherm imagery highlights elements in the scene that become lost in background clutter in the thermal image.

Figure 9. Scene showing thermal on the left and eTherm on the right. This scene shows detection of targets that are obscured (center) and of low thermal contrast (bottom left).

3.0 Summary

In this paper we have presented the Pyxis® LWIR 640 imaging polarimeter. It is a division of focal plane LWIR polarimeter built on an uncooled microbolometer with a low SWAP and provides a variety of output data products in both analog and digital formats in real time. Output data includes conventional thermal imagery, the linear elements of the Stokes vector, degree of linear polarization, and the eTherm image that incorporates all of this information and the polarization orientation. The functionality and SWAP makes the Pyxis® an attractive alternative to uncooled targeting sensors currently in use.

---

[1] Jacob L. Michalson; Joao M. Romano; Luz Roth; Stokes vector analysis of LWIR polarimetric in adverse weather. Proc. SPIE 8160, Polarization Science and Remote Sensing V, 81600N (September 9, 2011); doi:10.1117/12.893708.

[2] Bradley M. Ratliff; J. Scott Tyo; Wiley T. Black; James K. Boger; David L. Bowers; Polarization visual enhancement technique for LWIR microgrid polarimeter imagery. Proc. SPIE 6972, Polarization: Measurement, Analysis, and Remote Sensing VIII, 69720N (March 31, 2008); doi:10.1117/12.783079.

[3] M. Felton; K. P. Gurton; J. L. Pezzaniti; D. B. Chenault; L. E. Roth; Comparison of the inversion periods for MidIR and LWIR polarimetric and conventional thermal imagery. Proc. SPIE 7672, Polarization: Measurement, Analysis, and Remote Sensing IX, 76720R (April 26, 2010); doi:10.1117/12.850264.

[4] Joao M. Romano; Melvin Felton; David Chenault; Brian Sohr; Polarimetric imagery collection experiment. Proc. SPIE 7696, Automatic Target Recognition XX; Acquisition, Tracking, Pointing, and Laser Systems Technologies XXIV; and Optical Pattern Recognition XXI, 769611 (May 12, 2010); doi:10.1117/12.849911.

[5] Kristan Gurton; Melvin Felton; Robert Mack; Daniel LeMaster; Craig Farlow; Michael Kudenov; Larry Pezzaniti; MidIR and LWIR polarimetric sensor comparison study. Proc. SPIE 7672, Polarization: Measurement, Analysis, and Remote Sensing IX, 767205 (April 24, 2010); doi:10.1117/12.850341.

[6] John Harchanko; David Chenault; Craig Farlow; Kevin Spradley; Detecting a surface swimmer using long wave infrared imaging polarimetry (Invited Paper). Proc. SPIE 5780, Photonics for Port and Harbor Security, 138 (May 25, 2005); doi:10.1117/12.603874.

[7] John S. Harchanko; David B. Chenault; Water-surface object detection and classification using imaging polarimetry. Proc. SPIE 5888, Polarization Science and Remote Sensing II, 588815 (September 02, 2005); doi:10.1117/12.623542.

[8] Goldstein, D. *Polarized Light. 2nd Edition*. New York City: Marcel Dekker, Inc. 2003. Print.

[9] Balanis, C. *Advanced Engineering Electromagnetics*. Hoboken, NJ: John Wiley & Sons, Inc. 1989. Print

[10] Hecht, E. *Optics. 4th Edition*. San Francisco: Pearson/Addison Wesley. 2002. Print.

[11] Michelson, A. A. *Studies in Optics*. Ontario: General Publishing Company, Ltd. 1995. Print.

[12] J. Scott Tyo, Dennis L. Goldstein, David B. Chenault, and Joseph A. Shaw, "Review of passive imaging polarimetry for remote sensing applications," Appl. Opt. 45, 5453-5469 (2006); http://dx.doi.org /10.1364/AO.45.005453

[13] J. S. Tyo, E. N. Pugh, and N. Engheta, "Colorimetric Representations For Use With Polarization-Difference Imaging Of Objects In Scattering Media," J. Opt. Soc. Am. A **15**, 367–374 (1998).

[14] J. S. Tyo, et al., "The Effects of Thermal Equilibrium and Contrast in LWIR Polarimetric Images," Opt. Exp. **15 (**23), 15161-15167 (2007).